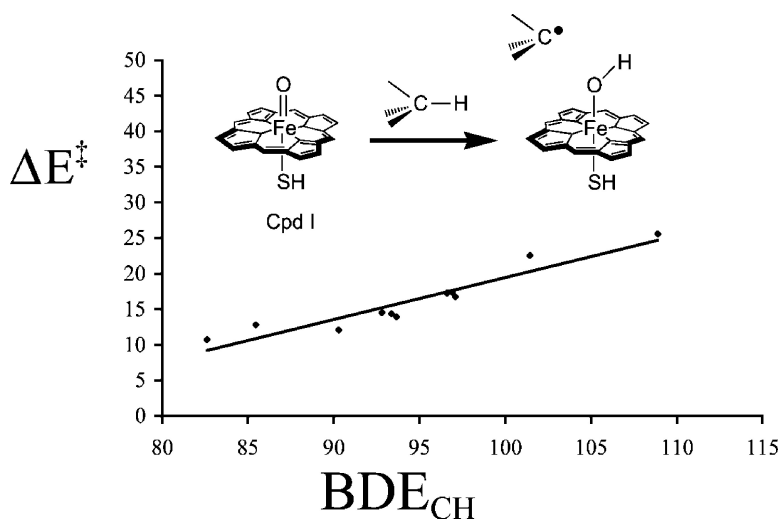


## A Predictive Pattern of Computed Barriers for C–H Hydroxylation by Compound I of Cytochrome P450

Sam P. de Visser, Devesh Kumar, Shimrit Cohen, Ronen Shacham, and Sason Shaik

*J. Am. Chem. Soc.*, **2004**, 126 (27), 8362-8363 • DOI: 10.1021/ja048528h • Publication Date (Web): 16 June 2004

Downloaded from <http://pubs.acs.org> on March 31, 2009



### More About This Article

Additional resources and features associated with this article are available within the HTML version:

- Supporting Information
- Links to the 8 articles that cite this article, as of the time of this article download
- Access to high resolution figures
- Links to articles and content related to this article
- Copyright permission to reproduce figures and/or text from this article

[View the Full Text HTML](#)

## A Predictive Pattern of Computed Barriers for C–H Hydroxylation by Compound I of Cytochrome P450

Sam P. de Visser, Devesh Kumar, Shimrit Cohen, Ronen Shacham, and Sason Shaik\*

Department of Chemistry and the Lise Meitner-Minerva Center for Computational Quantum Chemistry, The Hebrew University of Jerusalem, 91904 Jerusalem, Israel

Received March 14, 2004; E-mail: sason@yfaat.ch.huji.ac.il

There is growing interest in the enzyme cytochrome P450 and its ability to carry out the difficult process of hydroxylating nonactivated C–H bonds.<sup>1</sup> Despite this interest, barriers (and rate constants) for C–H bond activation by the enzyme are not available, and a full structure–reactivity picture is still lacking. Establishment of a predictive and reliable reactivity scale for different substrates would therefore be useful, both for a broad understanding of reactivity patterns and as input for kinetic modeling of experimental data.<sup>1c</sup> This paucity of experimental barriers may be filled initially by theoretical data derived from the best theoretical means. Currently, these exist in density functional theory (DFT).

The consensus active species of P450 is the high-valent iron(V)–oxo species, called Compound I (Cpd I, in Figure 1).<sup>1</sup> Korzekwa et al.<sup>2</sup> used a phenoxyl radical to model Cpd I and studied hydrogen abstraction (H-abstraction) reactions. Their semiempirical calculations showed correlations of the barriers with electronic factors including the C–H bond energy. Park and Harris<sup>3</sup> demonstrated that DFT calculations of the energetics of H-abstraction by Cpd I can predict the regiochemistry of substrate metabolism. Mayer et al.<sup>4</sup> showed that experimental barriers of H-abstractions, promoted by metal–oxo complexes, exhibit a linear correlation with the C–H bond energy as well as with the strength of the newly formed O–H bond, while Kaizer et al.<sup>5</sup> demonstrated such a correlation for C–H hydroxylation by a non-heme iron(IV)–oxo catalyst. Mayer<sup>4</sup> showed that these Bell–Evans–Polanyi-type correlations are universal and predictive. Furthermore, such correlations can be derived from fundamental models of barrier formation.<sup>6</sup> Therefore, the theoretical derivation of such structure–reactivity correlations should give one an opportunity to bracket barrier heights in the protein environment of P450.

Our previous DFT studies<sup>7</sup> of C–H hydroxylation by a model Cpd I species (Figure 1) are augmented here by six more cases resulting in barrier data for the following substrates: methane (**1**),<sup>7a</sup> propene (**2**),<sup>7b</sup> benzene (**3**),<sup>7c</sup> *trans*-1-methyl-2-phenyl cyclopropane (**4**),<sup>7d</sup> the *exo*-C5–H hydroxylation of camphor (**5**), ethane (**6**), the two different C–H positions of propane (**7n**, **7i**), *trans*-1-isopropyl-2-phenyl cyclo-propane (**8**),<sup>7d</sup> benzylic hydroxylation of toluene (**9**), and hydroxylation of the primary carbon of phenyl-ethane (**10**). This set is sufficiently large to establish a meaningful correlation.

The H-abstraction reactions of Cpd I were studied at the UB3LYP/LACVP level following previously described procedures.<sup>7</sup> Single-point calculations were carried out with the larger LACV3P+\* basis set. The C–H bond dissociation energies ( $BDE_{C-H}$ , eq 1) were calculated at the B3LYP/LACV3P+\*\*\* level (equivalent to 6-311++G\*\*) and compared well with experimental data (see Supporting Information). The effect of relaxation of the radical ( $RE_{Alk}$ ) on the  $BDE$ , was computed, as the energy difference of the  $Alk\cdot$  moiety in its geometry in  $Alk-H$  relative to its final

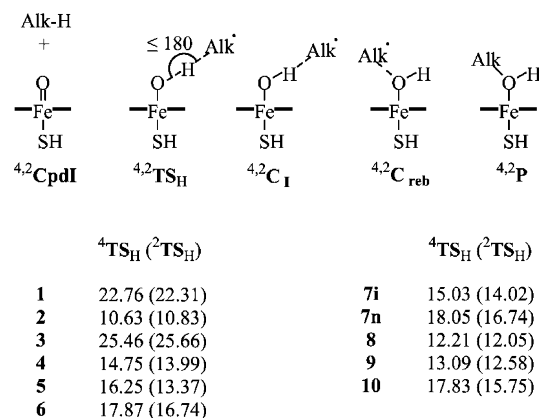
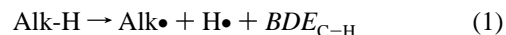


**Figure 1.** Computed species during C–H hydroxylation by Cpd I (the porphyrin is indicated by the bold lines) and UB3LYP/LACVP barrier data, ( $\Delta E^\ddagger(ZPE)$ ), in kcal mol<sup>-1</sup>, for substrates **1–10**.

optimized structure.



All the systems described here follow a two-state rebound mechanism, originating from the doublet and quartet ground states of Cpd I.<sup>7</sup> Generally, the rate-determining step involves H-abstraction via the transition states  ${}^4,2TS_H$ . The LACVP barriers after zero-point correction,  $\Delta E^\ddagger(ZPE)$  relative to isolated reactants are listed in Figure 1, for **1–10**.

We tested many different permutations of plotting the barrier heights as a function of C–H bond activation energy, see Supporting Information. Excellent linear correlations ( $R^2 = 0.98–0.99$ ) are obtained for the plot of the LACVP barriers against  $BDE_{C-H} - RE_{Alk}$ , for both spin states. Good correlations are also obtained for the reaction energy for the H-abstraction step (from **Cpd I** to **C<sub>I</sub>**, Figure 1). The effect of the basis set is limited since the LACV3P+\* barriers correlate well with the LACVP data ( $R^2 = 0.968$ ). Similarly, the  $\Delta H^\ddagger$  values that differ from  $\Delta E^\ddagger(ZPE)$  data by 0.0–0.4 kcal mol<sup>-1</sup> give equally good correlations. In fact, as shown in the Supporting Information, various permutations of the plots show good correlations. These correlations mean that the B3LYP/LACVP procedure gives a physically sensible set of transition states and barrier trends. A systematic error certainly exists since, the LACV3P+\* barriers are lower on average, by 1.2 kcal mol<sup>-1</sup>. While this may change with geometry optimization and a still better basis set, it is not likely to change much more. For practical purposes we need a plot that can be used across the board by reliance on only experimental  $BDE_{CH}$  data. Figure 2 is such a plot of the computed averaged high-spin and low-spin  $\Delta E^\ddagger(ZPE)$  barriers against the experimentally matched  $BDE(ZPE)_{CH}$  values. The trend shows clearly an increase of barrier height with increased

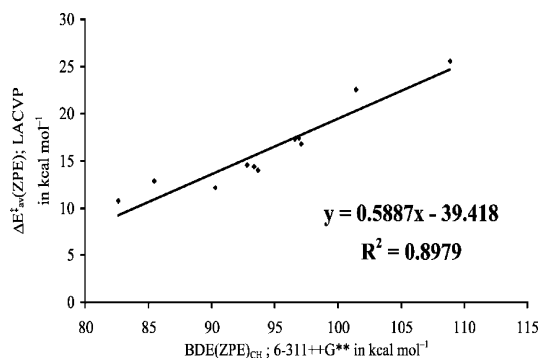


**Figure 2.** Averaged and ZPE-corrected H-abstraction barriers (in kcal mol<sup>-1</sup>) for the reaction of <sup>4,2</sup>Cpd I + Alk-H (Alk-H = **1–10**) as a function of  $BDE(ZPE)_{CH}$ .

C–H bond energy. The equation of the line can be used to bracket barriers within 1–2 kcal mol<sup>-1</sup>.

To test the utility of the correlation in Figure 2, we used Mayer's C–H bond energy data,<sup>4b</sup> for the series PhCH<sub>3</sub>, Ph<sub>2</sub>CH<sub>2</sub>, Ph<sub>3</sub>CH, 9,10-dihydroanthracene, and xanthene, to calculate corresponding  $\Delta E^\ddagger(ZPE)$  values. Since the difference of the  $BDE_{CH}$  values across this Mayer series is 14.4 kcal mol<sup>-1</sup>, the theoretical equation predicts a barrier difference of 8.5 kcal mol<sup>-1</sup>, while the experimental difference<sup>4b</sup> obtained for oxidation by KMnO<sub>4</sub> is 9.3 kcal mol<sup>-1</sup>. Our calculated barriers are lower than Mayer's  $\Delta H^\ddagger$  data, and at least part of this difference is accountable by the stronger FeO–H bond, made by Cpd I, relative to the KMnO<sub>4</sub> oxidant used in the Mayer series. Thus, our datum is  $BDE(ZPE)_{FeO-H} = 87.9$  kcal mol<sup>-1</sup> (LACV3P+\*), while Mayer's  $BDE_{MnO-H} \approx 80$  kcal mol<sup>-1</sup>. Applying the equation of Figure 2 to the difference of these bond energies increases the calculated barriers by 4.7 kcal mol<sup>-1</sup> and brings them closer to Mayer's  $\Delta H^\ddagger$  data to within 2–4 kcal mol<sup>-1</sup>, reasonably close within the scatter in the experimental data and the theoretical plot. Another comparison is with the experimental barriers for hydroxylation by Cpd I-like porphyrin–Mn(V)–oxo species, in acetonitrile.<sup>8</sup> Thus, using the C–H bond energy for Ph<sub>2</sub>CH<sub>2</sub> (82 kcal mol<sup>-1</sup>), and assuming the same MnO–H bond energy as for FeO–H, the equation in Figure 2 predicts a barrier of 8.6 kcal/mol, compared with ~11–13 kcal mol<sup>-1</sup> with three different Mn(V)–oxo species. Other series with similar performance (Tables S.6–S.8) show the utility of the correlating equation in Figure 2.

Let us turn now to barriers inside the active site of P450 enzymes. As was argued recently,<sup>9</sup> the enzyme absorbs the entropic cost of substrate binding by release of water molecules from the binding site, and therefore, a better estimate of the reaction free energy barrier would be the quantity measured from the substrate–enzyme complex to the transition state.<sup>10</sup> Thus, our  $\Delta E^\ddagger(ZPE)$  or  $\Delta H^\ddagger$  data can be used to represent the  $\Delta G^\ddagger$  for the reaction in the pocket of the enzyme.

Camphor hydroxylation by P450<sub>cam</sub> has iconic importance. Our low-spin  $\Delta E^\ddagger(ZPE)$  barriers, from the cluster, are 16.5 (LACVP) and ~15.1 (LACV3P+\*) kcal mol<sup>-1</sup>, and the  $\Delta H^\ddagger$  values are within 0.4–0.6 kcal mol<sup>-1</sup>. These values are very close to the recent  $\Delta E^\ddagger(ZPE)$  barrier data computed by QM/MM calculations.<sup>9</sup> The

$BDE(ZPE)_{CH}$  value for camphor is 93.7 kcal mol<sup>-1</sup>. Using the Mayer series,<sup>4a</sup> with CrO<sub>2</sub>Cl<sub>2</sub> as the oxidant, we find that C<sub>8</sub>H<sub>16</sub> with  $BDE_{CH} = 95.7$  kcal mol<sup>-1</sup> (C<sub>8</sub>H<sub>16</sub>) gave a  $\Delta H^\ddagger$  value of 19.4 kcal mol<sup>-1</sup>. Taking into account the  $BDE_{CH}$  differences and the fact that the calculated FeO–H bond energy is stronger than the estimated<sup>4a</sup> one for CrO–H by 5 kcal mol<sup>-1</sup>, we would expect a lower barrier for camphor hydroxylation by Cpd I. From the slope of the correlation in Figure 2, the barrier lowering should be 4.1 kcal mol<sup>-1</sup>, thereby leading to “an experimentally scaled barrier” for camphor hydroxylation of 15.4 kcal mol<sup>-1</sup>. Using the porphyrin–Mn(V)–oxo data,<sup>8</sup> in conjunction with the correlation in Figure 2, leads to another “experimentally scaled barrier” of 17.7 kcal mol<sup>-1</sup> for camphor hydroxylation. A single-turnover kinetics datum for camphor hydroxylation by P450<sub>cam</sub><sup>11</sup> yields an upper limit of the free energy barrier as  $\Delta G^\ddagger < 15$  kcal/mol ( $k > 200$  s<sup>-1</sup>). The theoretically computed barriers (e.g., 15.1 kcal mol<sup>-1</sup>, LACV3P+\*) are not too far from these values. Thus, the correlating equation appears to make reasonable estimates of the barriers. Nevertheless, the fact that Cpd I of P450<sub>cam</sub> has not yet been detected under normal working enzymatic conditions<sup>12</sup> would seem to require a significantly lower barrier for camphor hydroxylation. Possible reasons for barrier lowering to seek are tunneling<sup>5,9</sup> or entropic reduction due to increased protein degrees of freedom during the H-abstraction TS.

In summation we showed here an extended barrier–bond energy correlation for C–H hydroxylation by P450. A single experimental datum can anchor this theoretical correlation.

**Acknowledgment.** The research was supported by a grant from the Israeli Science Foundation (ISF).

**Supporting Information Available:** Eight tables and 30 figures of  $BDE$  data and results on C–H hydroxylation. This material is available free of charge via the Internet at <http://pubs.acs.org>.

## References

- (1) (a) Ortiz de Montellano, P. R.; De Voss, J. J. *Nat. Prod. Rep.* **2002**, *19*, 1. (b) Groves, J. T. *Proc. Natl. Acad. Sci. U.S.A.* **2003**, *100*, 3569. (c) Guengerich, F. P. *Chem. Res. Toxicol.* **2001**, *14*, 611.
- (2) Korzekwa, K. R.; Jones, J. P.; Gillette, J. R. *J. Am. Chem. Soc.* **1990**, *112*, 7042.
- (3) Park, J.-Y.; Harris, D. L. *J. Med. Chem.* **2003**, *46*, 1645.
- (4) (a) Mayer, J. M. *Acc. Chem. Res.* **1998**, *31*, 441. (b) Mayer, J. M. In *Biomimetic Oxidations Catalyzed by Transition Metal Complexes*; Meunier, B., Ed.; Imperial College Press: 1999; p 1.
- (5) Kaizer, J.; Klinker, E. J.; Oh, N. Y.; Rohde, J.-U.; Song, W. J.; Stubna, A.; Kim, J.; Münck, E.; Nam, W.; Que, L., Jr. *J. Am. Chem. Soc.* **2004**, *126*, 472.
- (6) Shaik, S.; Shurki, A. *Angew. Chem., Int. Ed.* **1999**, *38*, 586.
- (7) (a) Ogliaro, F.; Harris, N.; Cohen, S.; Filatov, M.; de Visser, S. P.; Shaik, S. *J. Am. Chem. Soc.* **2000**, *122*, 8977. (b) de Visser, S. P.; Ogliaro, F.; Sharma, P. K.; Shaik, S. *J. Am. Chem. Soc.* **2002**, *124*, 11809. (c) de Visser, S. P.; Shaik, S. *J. Am. Chem. Soc.* **2003**, *125*, 7413. (d) Kumar, D.; de Visser, S. P.; Shaik, S. *J. Am. Chem. Soc.* **2004**, *126*, 1907.
- (8) Zhang, R.; Newcomb, M. *J. Am. Chem. Soc.* **2003**, *125*, 12418.
- (9) Schöneboom, J. C.; Cohen, S.; Lin, H.; Shaik, S.; Thiel, W. *J. Am. Chem. Soc.* **2004**, *126*, 4017.
- (10) See related conclusion: Bassan, A.; Blomberg, M. R. A.; Siegbahn, P. E. M. *Chem.-Eur. J.* **2003**, *9*, 4055.
- (11) Brewer, C. B.; Peterson, J. A. *J. Biol. Chem.* **1988**, *263*, 791.
- (12) Kellner, D. G.; Hung, S. C.; Weiss, K. E.; Sligar, S. G. *J. Biol. Chem.* **2002**, *277*, 9641.

JA048528H